NANO LETTERS

LETTER

pubs.acs.org/NanoLett

Strongly Enhanced Molecular Fluorescence inside a Nanoscale Waveguide Gap

Volker J. Sorger,[†,∥] Nitipat Pholchai,[†,∥] Ertugrul Cubukcu,[†,∥] Rupert F. Oulton,[†] Pavel Kolchin,[†] Christian Borschel,[§] Martin Gnauck,[§] Carsten Ronning,[§] and Xiang Zhang*[,†,‡]

[†]NSF Nanoscale Science and Engineering Center, 3112 Etcheverry Hall, University of California, Berkeley, California 94720, United States

[‡]Materials Sciences Division, Lawrence Berkeley National Laboratory, 1 Cyclotron Road, Berkeley, California 94720, United States

[§]Institute for Solid State Physics, Friedrich-Schiller-University Jena, Max-Wien-Platz 1, 07743 Jena, Germany

Supporting Information

ABSTRACT: We experimentally demonstrate dramatically enhanced light−matter interaction for molecules placed inside the nanometer scale gap of a plasmonic waveguide. We observe spontaneous emission rate enhancements of up to about 60 times due to strong optical localization in two dimensions. This rate enhancement is a nonresonant nature of the plasmonic waveguide under study overcoming the fundamental bandwidth limitation of conventional devices. Moreover, we show that about 85% of molecular emission couples into the waveguide highlighting the dominance of the nanoscale optical mode in competing with quenching processes. Such optics at molecular length scales paves the way toward integrated on-chip photon source, rapid transfer of quantum information, and efficient light extraction for solid-state-lighting devices.

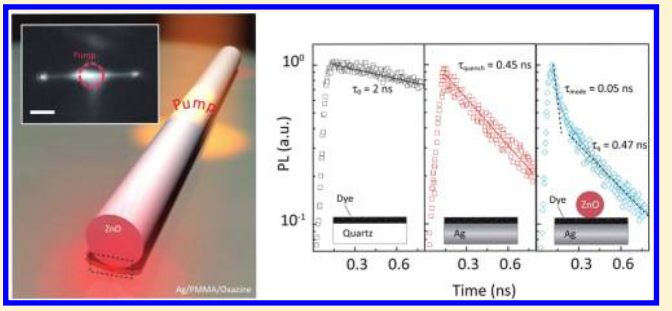

KEYWORDS: Plasmonic, waveguide, nanophotonics, molecular, fluorescence, Purcell

Nanophotonics research aims to study compact optoelectronic device architectures that scale on par with digital electronics by exploiting light beyond the diffraction limit.[1−5] Most importantly, device miniaturization also strengthens intrinsically weak light−matter interactions toward faster, more efficient, and novel optoelectronic functionalities.[4−6] These inherently weak interactions between light and matter are due to the vast difference in the characteristic wavelengths of light and electrons. A well-known solution is to place emitters within an optical cavity with a small optical mode volume and high Q-factor.[1] However, as long as optical cavities remain diffraction limited, strong light−matter interactions will rely on high quality factors (Q-factors),[7−10] which impose intrinsic limits on emission rates and bandwidths and often require painstaking tuning of emitter and cavity resonances.[11] The remaining strategy, to utilize electromagnetic field enhancement by reducing the spatial size of optical modes beyond the diffraction limit, is appealing because it allows for strong light−matter interactions with extremely low Q-factor systems.[12−14] Hence, even the low densities of states of confined propagating waves are sufficient to significantly strengthen light−matter interactions.[2−5]

In this Letter, we report large enhancements of the spontaneous rate of molecular emission inside a nanoscale waveguide gap and strong emission coupling to the deep subwavelength propagating plasmonic waveguide mode.[15,16] This hybrid plasmon polariton (HPP) waveguide mode is henceforth called HPP mode. We measure a reduction in emission lifetimes by as much as 60 times relative to the intrinsic lifetime of dye molecules over the broad spectral bandwidth of emission (>70 nm). We attribute the high Purcell factors to a number of generated emission modes since the molecules probe the local density of states of the waveguide.[1] Furthermore, we observe a 5-fold enhancement of the overall photoluminescence (PL) rate indicative of successful competition of the subwavelength gap mode with other emission channels. These results signify a high (up to 85%) probability that the molecular emission can be launched into the ultrasmall HPP waveguide mode. Such efficient coupling of emission into waveguiding structures holds promise for the transfer of quantum information technology,[17] the efficient light extraction[18,19] beyond the cavity-limited bandwidth, and the speed of photonics.[20,21]

In our experiments, we fabricated waveguides consisting of high permittivity ZnO semiconductor nanowires[22] (n = 2) separated from a thick silver film by a low permittivity PMMA layer (n = 1.46) of controllable nanoscale thickness containing Oxazine dye molecules,[23] as shown in Figure 1a,b.[15,16] The nanowire diameters were chosen to give an optimum confinement.[4,15] The silver was evaporated onto a quartz substrate while the Oxazine/PMMA and nanowires were spin-coated from solution. The silver film was optimized for smoothness in the evaporation step and showed a roughness of about 0.5 nm (rms) after deposition.

Received: August 15, 2011
Revised: September 25, 2011
Published: October 06, 2011

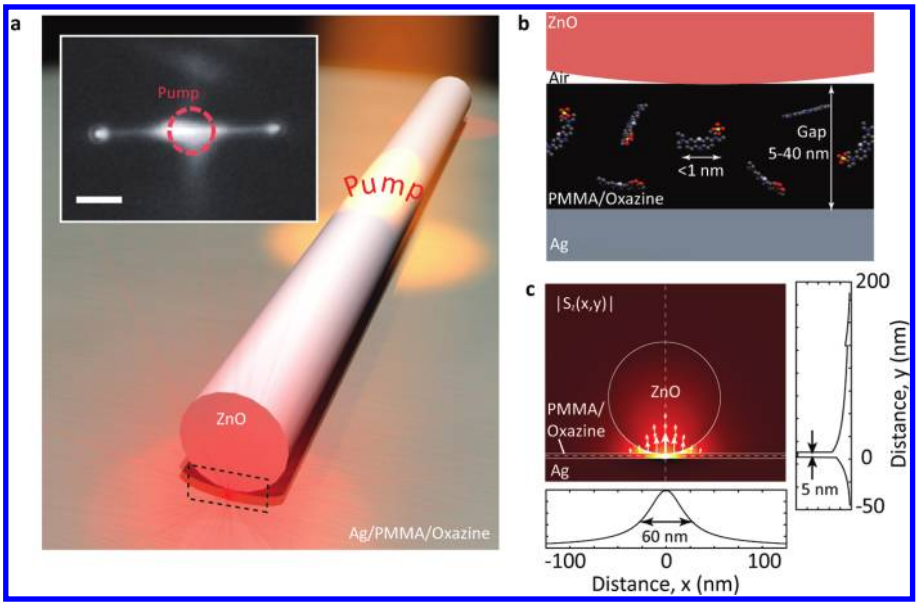

Figure 1. (a) Schematic of the waveguide with dye-doped PMMA films (nanowire diameter = 80−160 nm, length about 5 μm). Dye to PMMA ratio = 0.06 wt %. Inset, photoluminescence (PL) image of emission from dye molecules excited at the center of the nanowire (red circle) coupling to the deep subwavelength waveguide mode, and scattering to far field at the ends of the waveguide. Scale bar = 2 μm. (b) Zoom-in of the dashed rectangle area in panel a highlighting the critical nanoscale gap of this mode waveguide. (c) Waveguide mode's pointing vector, $|S_z(x,y)|$ supporting a deep subwavelength propagating mode (full width at half-maximum = 5 and 60 nm in x and y directions, respectively).[17,18].

The resulting deep subwavelength confinement in the gap layer arises from the hybridization of the photonic mode of the nanowire and a surface plasmon polariton; polarization surface charge on the semiconductor nanowire and collective electron oscillations on the metal interface sustain a strong electric field in the dye region that is perpendicular to the substrate forming the HPP waveguide mode,[15,16] as shown in Figure 1c. Key to this configuration is the placement of the dye emitters in the waveguide mode's region of highest electric field intensity, as described above.[15,16] Notice, the PL emission from nanowire defect states at low pump powers was found to be insignificant compared to the PL signal from the dye molecules. First evidence of efficient coupling between the dye molecules and the guided mode is fluorescence from the waveguide ends; emission from optically excited molecules beneath the middle of the waveguide propagates and subsequently scatters from the two nanowire ends (inset Figure 1a).

For the emitting dye molecules we chose a strong emitting molecule Oxazine (O1 perchlorate 750) which absorbs in the visible green spectrum and emits in the visible red region (Figure 2a,b). To demonstrate strongly coupled dye molecule emission into the deep subwavelength guided HPP mode, we choose to utilize a time-resolved spontaneous emission spectroscopy (Figure 2c). We measured the spontaneous emission lifetime using time-correlated single photon counting (TCSPC system PicoQuant), where the dye molecules were excited by femtosecond laser pulses (Ti:sapphire femtosecond pulse laser, λ = 620 nm, spot radius ~1 μm, femtosecond pulse length ~100 fs) focused to a spot of about 2 μm diameter onto the longitudinal midpoint of each waveguide (objective lens 63×, NA = 0.95). Spontaneous emission of the dyes was collected by the same objective, filtered within the spectrum bandwidth of 633−700 nm and registered by an avalanche photodiode. Note, the detector's (APD, MicroPhotonicDevices, PDM-series) dark count rate is one-tenth of

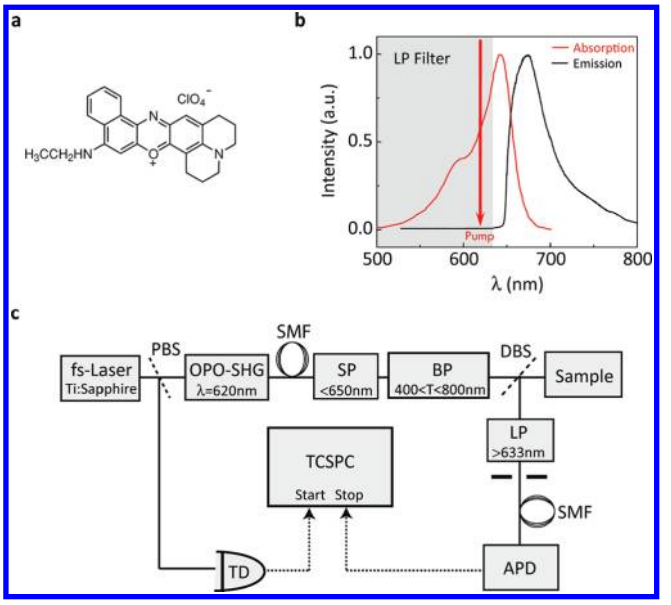

Figure 2. (a) Chemical structure of Oxazine (O1 perchlorate 750) dye molecule. (b) Measured spectral emission and absorption (after ref 24) of the Oxazine dyes in a PMMA host matrix. (c) Schematic of the micro-photoluminescence time-correlated single photon counting (TCSPC) setup: Ti:sapphire femtosecond-pulse laser, pulse width ~100 fs; PBS, polarizing beam splitter; OPO, optical parametric amplifier; SHG, second harmonic generation; SMF, single mode fiber for spatial filtering; SP/BP/LP, short-pass/bandpass/long-pass filters; DBS, dichroic beamsplitter (long pass edge = 625 nm); APD, avalanche photodiode; TCSPC. time-correlated single-photon counting system (Pico-quant); TD. trigger diode.

the photon collection rate from samples with dye molecules; thus no instrument response artifacts are expected in the single photon counting data. The dye emission at the detector of the

dx.doi.org/10.1021/nl202825s |Nano Lett. 2011, 11, 4907–4911

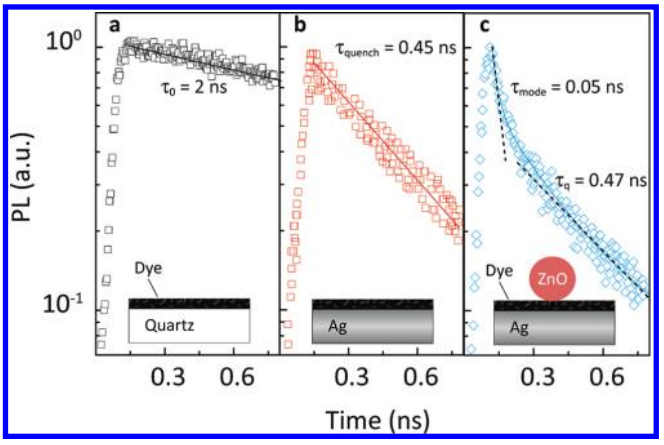

Figure 3. (a) PL decay histograms with insets showing corresponding sample schematics (dye:PMMA thickness, g = 10 nm). (a, b) Control samples (i) and (ii) serving as the intrinsic decay and quenched decay references, with average count rates of about 10^4 and 10^3 s^{-1}, respectively. (c) The subwavelength mode waveguide sample yields a shorter lifetime component due to coupling to a subwavelength waveguide mode (nonresonant Purcell effect), while the longer lifetime is due to uncoupled background molecules offset from the nanowire, which is consistent with the lifetimes observed in (b). Average count rate was about 10^3 s^{-1}. Dashed lines are guides to the eye for the two exponential dependencies.

setup is shown in Figure 2b, whereas the absorption was taken from ref 23. The emission is relatively broad band with a spectral width of about 70 nm (fwhm).

From the collected emission at the nanowire ends, time delayed histograms were build up using the delay between laser pulses and detected photons (Figure 3). Spontaneous emission lifetimes were extracted by fitting the time response histogram to a biexponential lifetime model, which was sufficient to describe the spatial and dipole orientation heterogeneity between the optical mode and background dye emission. To gain insight into the emission coupling to the various decay channels, we fabricated two control samples consisting of a 10 nm thick Oxazine/PMMA layer spin-coated onto (i) quartz and (ii) silver (300 nm). Control (i) serves as a reference for the average intrinsic spontaneous emission lifetime of dye molecules in PMMA ($\tau_{(i)} = \tau_0 = 2$ ns, Figure 3a). Control (ii), on the other hand, quantifies coupling to in-plane surface plasmons and the nonradiative quenching to the metal, which dominate over coupling to free space resulting in shorter lifetimes ($\tau_{(ii)} = 0.45$ ns, Figure 3b). The spontaneous emission lifetimes of the control samples are in sharp contrast to those of dye emission from the waveguide mode configuration with a 10 nm Oxazine/PMMA layer yielding the shortest lifetimes ($\tau_m = 48 \pm 12$ ps, Figure 3c). The enhancement beyond that of control (ii) arises from the strong mode confinement and suggests that the majority of emitted photons couple to the waveguide mode. Further evidence for the role of the waveguide mode in the emission process is seen in the shapes of the time delay histograms in Figure 3. While both histograms for the two control samples display single exponential decays, the waveguide's histogram is biexponential. However, coupling of dye molecules to the waveguide mode depends on both the position beneath the nanowire and the dipole orientation, since the mode is laterally confined and polarized perpendicular to the metal surface (Figure 3c). We therefore attribute the observed biexponential decay of dye emission in the waveguide structure to the different decay rates of coupled (fast decay) and uncoupled (slow decay) molecules to the deep subwavelength waveguide mode (see Supporting Information). This conclusion is supported by the observation that the slower decay rate is comparable to the decay rate of the dye in control (ii).

To understand the mechanism of strong coupling of dye emission to the waveguide mode in more detail, we have conducted the experiments above for various Oxazine/PMMA layer thicknesses, g. Panels a and b of Figure 4 show a schematic of the possible decay channels and the measurement results, respectively, highlighting two distinct trends with changing g for the emission rate into the waveguide mode and nonradiative quenching (**Q** for quenching and **M** for waveguide mode in Figure 4b). The experimental data from the spontaneous lifetime measurements (squares) for varying dye/PMMA thickness, g, agree well with the theoretically predicted (lines) total decay rate of a single dipole in both control (ii) (red squares and red dashed line) and the HPP mode (black squares and black solid line, Figure 4b). Notice, these results required dye molecules that were not coupled to the waveguide to be removed, since their emission mask the signal from the HPP mode for large gaps, g, as exemplified in Figure 4c (see Supporting Information). The origin of this masking-effect comes from the size discrepancy between the collection area ($\sim$1 μm), the nanowire diameter ($\sim$100 nm), and subsequent dye emission collection efficiencies. We effectively eliminated this problem by deploying a mild oxygen plasma treatment removing the uncoupled dye molecules, where the nanowires themselves act as an etch mask (Figure 4c). Lifetime measurements of samples before and after etching showed single exponential decay histogram with $\tau_{before} = 1.0$ ns and $\tau_{after} = 0.4$ ns, respectively, e.g., for g = 20 nm. Eliminating the overshadowing background signal contribution for large g, we are able to extract the total Purcell factor (Figure4b, black squares), which matchs the predicted curve well (Figure 4b black solid line). In contrast, repeating the etch process step for small gap sizes did reveal a biexponential decay before and after etching, showing the contributions of the vertical dipole and quenching. The reason behind these two different displays is the very strong Purcell factor at low gap sizes. In other words, the background no longer dominates in this low-g regime (g < 10 nm), which confirms the proper operation of the HPP mode, providing strong Purcell enhancements due to the subwavelength scale optical mode.

Furthermore, we were interested in investigating where the emission ends up; a question that is guided by an analysis of the rate enhancement factor, F. While the enhancement factor for control (ii), $F_{(tt)}(g) = F_{Rad}(g) + F_{spp}(g) + F_q(g)$, includes the contributions from emission into radiation waves, $F_{spp}(g)$, surface plasmons, and nonradiative quenching, $F_q(g)$, the enhancement factor for the nanowire sample, $F_p(g)$, also includes the contribution of the waveguide mode, i.e., $F_{(m}(g) \approx F_p(g) - F_{(tt)}(g)$. This provides an estimate of the waveguide mode coupling probability, $\beta(g) \approx 1 - F_{(tt)}(g)/F_p(g)$ (Figure 5), suggesting that emission into the hybrid plasmon mode dominates over all the other emission channels for a large range gap sizes, g[15,16] with β-factors as high as 85%. However, for gaps smaller than about 5 nm, nonradiative quenching starts to dominate over emission into the waveguide mode (red squares) and the β-factor approaches zero (Figure 5). Note, that horizontal dipole components display no modal Purcell effect ($F_m < 1$) anywhere underneath the waveguide. As a result their decay is dominated by nonradiative quenching at small gap such that their

dx.doi.org/10.1021/nl202825s |*Nano Lett.* 2011, 11, 4907–4911

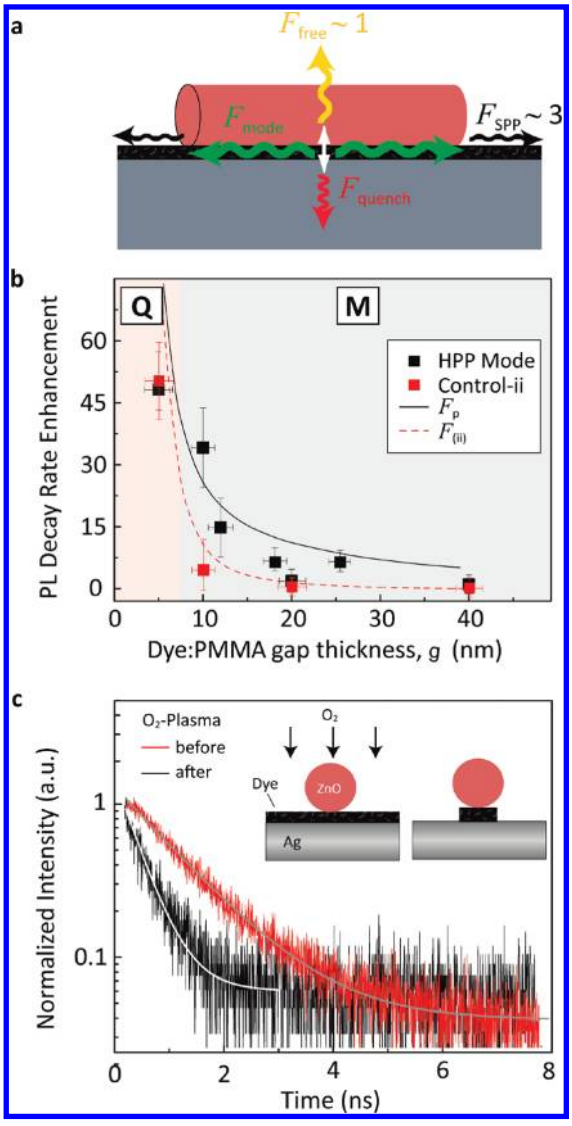

Figure 4. (a) Possible decay channels: the nanoscale waveguide mode, free space, surface plasmon, and quenching. The white arrow indicates the position of the molecular dipole emitters. (b) Average measured and calculated (see Supporting Information) spontaneous decay rate enhancements versus gap thickness, g, highlighting competition between the various decay channels. Quenching dominates for $g < 8$ nm (region **Q**), while preferential coupling to the nanoscale waveguide mode is achieved for $g > 8$ nm (region **M**). An average (highest) enhancement of 48 (60) is observed at $g = 5$ nm. For large g (>20 nm) the theoretically predicted trend of F_p is found by reducing the molecular background emission signal via O_2-plasma etching using the nanowire as a mask (see Supporting Information). In the calculations, the emitting dipole (black vertical arrow in panel a is positioned midgap ($g/2$), nanowire diameter, $d_{NW} = 120$ nm. (c) Selective removal of dye molecules not coupled to the HPP waveguide mode. The nanowire is used as a shadow mask to etch the dye layer via a mild O_2-plasma treatment (Inset). For large gap sizes, the decay histograms show a single exponential decay before and after etching, however, with long (short) lifetimes before (after) etching. The long lifetime response before etching stems from uncoupled molecular emission creating a background signal overshadowing the HPP mode channel.

mode coupling factor and intensity is nearly undetectable, thereby allowing us to distinguish clearly the coupling effect on vertical dipoles (see Supporting Information). In addition to

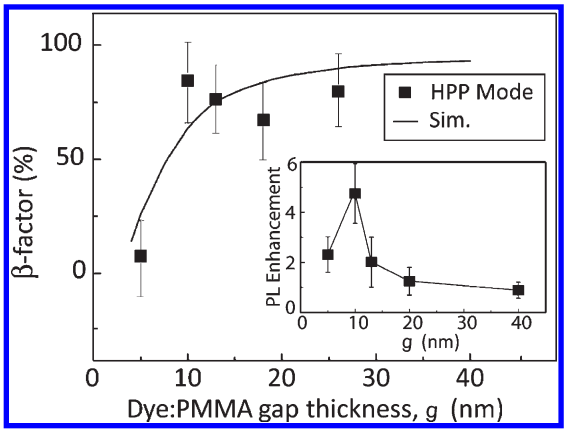

Figure 5. The waveguide mode's β-factor increases monotonically with gap thickness, g, over the range shown and dominates other emission channels for $g > 8$ nm. Note, for data points at $g = 18, 26$ nm, interpolation between neighboring data points from control (ii) was used. Inset, measured PL enhancement (photon flux from HPP mode vs plasmonic control-ii) showing the successful competition of the nanoscale mode over other emission channels resulting in a 5-fold increase.

the enhancement of the spontaneous emission lifetime, the PL brightness, or photon flux, at the detector is important from a practical device consideration, e.g., light emitting or detecting device.[18,19] We benchmarked the total photon flux from the HPP waveguide design (pump on nanowire) against a pure plasmonic case (pump on metal = control-ii). By varying the gap thickness we observed a 5-fold PL enhancement around $g = 10$ nm (inset Figure 5). This enhancement ratio of PL extraction is related to the product of the spontaneous emission rate enhancement (F_p) and the spontaneous emission factor (β) of the deep subwavelength waveguide mode, while $\beta F_p = F_m$, should be a monotonic function of the gap width, at least for this range values, the PL enhancement appears to peak near $g = 10$ nm.

To summarize, we have experimentally proven enhanced optical emission at molecular length scales toward strong and efficient light−matter interactions. We have quantitatively measured the spontaneous decay rate and PL intensity enhancement of dye molecules, which sample the subwavelength mode area in the nanoscale gap region of a hybrid plasmon waveguide. We show that 85% of the molecular emission can be coupled to an optical waveguide with deep subwavelength confinement and verify the metal quenching contribution in the PL decay data. Furthermore, we verify successful competition of the nanoscale waveguide mode with other loss channels by reporting a PL brightness enhancement up to 5-fold for an optimum gap height of about 10 nm. Such optics at molecular length scales guide the way to a deeper understanding and improved control of coupling between emission and waveguide architectures toward the development of rapid transfer of quantum information[17] and efficient light extraction[18,19] beyond the cavity-limited bandwidth[7,8,10,20,21] as well as integrated on-chip photon source.[24]

■ ASSOCIATED CONTENT

Supporting Information. Calculation of the modal Purcell factor, rate enhancement breakdown by emission channel, nanowire emission control, and effect of dipole orientation on modal Purcell factor. This material is available free of charge via the Internet at http://pubs.acs.org.

dx.doi.org/10.1021/nl202825s |*Nano Lett.* 2011, 11, 4907–4911

AUTHOR INFORMATION

Corresponding Author
*E-mail: xiang@berkeley.edu.

Author Contributions
‖These authors contributed equally.

ACKNOWLEDGMENT

We acknowledge support from the National Science Foundation (NSF) Nanoscale Science and Engineering Center (SINAM, CMMI-0751621).

REFERENCES

(1) Purcell, E. M. *Phys. Rev.* **1946**, *69*, 681.
(2) Stockman, M. I. *Phys. Today* **2011**, 39–44.
(3) Chang, D. E.; Sørensen, A. S.; Hemmer, P. R.; Lukin, M. D. *Phys. Rev. Lett.* **2006**, *97*, 053002.
(4) Oulton, R. F.; Sorger, V. J.; Zentgraf, T.; Gladden, C.; et al. *Nature* **2009**, *461*, 629.
(5) Jun, Y. C.; Huang, K. C. Y.; Brongersma, M. L. *Nat. Commun.* **2011**, *2*, 283.
(6) Zentgraf, T.; Liu, Y.; Mikkelsen, M. H.; Valentine, J.; Zhang, X. *Nat. Nanotechnol.* **2011**, *6*, 151.
(7) Pinkse, P. W. H.; Fischer, T.; Maunz, P.; Rempe, G. *Nature* **2000**, *404*, 365–368.
(8) Peter, E.; Senellart, P.; Martrou, D.; Lemaıtre, A.; et al. *Phys. Rev. Lett.* **2005**, *95*, 067401.
(9) Gontijo, I.; Boroditsky, M.; Yablonovitch, E. *Phys. Rev. Lett.* **1999**, *60*, 11564.
(10) Chang, D. E.; Sorensen, A. S.; Demler, E.; Lukin, M. D. *Nat. Phys.* **2007**, *3*, 807.
(11) Faraon, A.; Englund, D.; Bulla, D.; Luther-Davies, B.; et al. *Appl. Phys. Lett.* **2008**, *92*, 043123.
(12) Anger, P.; Bharadwaj, P.; Novotny, L. *Phys. Rev. Lett.* **2006**, *96*, 113002.
(13) Kinkhabwala, A.; Yu, Z; Fan, S; Avlasevich, Y.; et al. *Nature* **2008**, *443*, 1062.
(14) Utikal, T.; Stockman, M. I.; Heberle, A. P.; Lippitz, M.; et al. *Phys. Rev. Lett.* **2010**, *104*, 113903.
(15) Oulton, R. F.; Sorger, V. J.; Genov, D. A.; Pile, D. F. P.; et al. *Nat. Photonics* **2008**, *2*, 495–500.
(16) Sorger, V. J.; Ye, Z.; Oulton, R. F; Wang, Y.; et al. *Nat. Commun.* **2011**, *2*, 331.
(17) Lukin, M. D.; Fleischhauer, M.; Cote, R.; Duan, L. M.; et al. *Phys. Rev. Lett.* **2001**, *87*, 037901.
(18) Fedutik, Y.; Temnov, V. V.; Schoeps, O.; Woggon, U. *Phys. Rev. Lett.* **2007**, *99*, 136802.
(19) Lund-Hansen, T.; Stobbe, S.; Julsgaard, B.; Thyrrestrup, H.; et al. *Phys. Rev. Lett.* **2008**, *101*, 113903.
(20) Lecamp, G.; Lalanne, P.; Hugonin, J. P. *Phys. Rev. Lett.* **2007**, *99*, 193901.
(21) Stockman, M. I. *New J. Phys* **2008**, *10*, 025031.
(22) Borchers, C.; Müller, S.; Stichtenoth, D.; Schwen, D.; et al. *J. Phys. Chem. B* **2006**, *110*, 1656.
(23) Zoriniants, G.; Barns, W. *New J. Phys.* **2008**, *10*, 105002.
(24) Liu, A.; Jones, R.; Liao, L.; Samara-Rubio, D.; Rubin, D.; et al. *Nature* **2004**, *427*, 615–619.